Journal of MATERIALS RESEARCH

Article
DOI: 10.1557/jmr.2019.303

EARLY CAREER SCHOLARS IN MATERIALS SCIENCE

ANNUAL ISSUE

Flexible low-voltage paper transistors harnessing ion gel/cellulose fiber composites

Xu Wang[1], Cunjiang Yu[2,a)]

[1]Materials Science and Engineering Program, University of Houston, Houston, Texas 77204, USA
[2]Department of Mechanical Engineering, Materials Science and Engineering Program, Department of Biomedical Engineering, Department of Electrical and Computer Engineering, Texas Center for Superconductivity, University of Houston, Houston, Texas 77204, USA
[a)]Address all correspondence to this author. e-mail: cyu15@uh.edu

Received: 2 June 2019; accepted: 16 September 2019

Paper transistors are indispensable devices for paper-based electronic biosensing systems. Existing paper transistors mainly use paper as a mechanical support in a passive fashion. By taking advantage of the cellulose fibers in paper, here we report a transistor-in-paper where paper is employed as an essential part to allow for low-voltage operation, which addresses the long-standing challenge of high-voltage operation with existing paper transistors. Such a low-threshold voltage is because of the ion gel/cellulose fiber composite dielectric formed by modifying the paper with ion gels. We further developed paper-based inverters as examples of logic gates and an integrated tactile sensing mat based on a transistor array–enabled multiplexing device. The results collectively indicate that the ion gel–modified paper leads to a class of flexible, low-voltage transistors and integrated electronic devices, which hold promise in many applications.

Cunjiang Yu

Dr. Cunjiang Yu is currently the Bill D. Cook Associate Professor of Mechanical Engineering at the University of Houston, with joint appointments in Electrical and Computer Engineering, Materials Science and Engineering, and Biomedical Engineering. He received his B.S. in Mechanical Engineering and M.S. in Electrical Engineering in 2004 and 2007, respectively, from Southeast University, Nanjing, China. He completed his Ph.D. in Mechanical Engineering at Arizona State University in 2010 and was trained as a postdoc at the University of Illinois at Urbana-Champaign before joining the University of Houston in 2013. Yu's research focuses on material design, manufacturing approaches, and device technologies toward soft electronics for a broad range of applications. Yu is a recipient of the National Science Foundation Faculty Early Career Development Program (NSF CAREER) Award, Office of Naval Research (ONR) Young Investigator Award, MIT Technology Review 35 Top Innovators under the age of 35—TR35 China, Society of Manufacturing Engineers (SME) Outstanding Young Manufacturing Engineer Award, American Vacuum Society Thin Film Division Young Investigator Awards, American Chemical Society Petroleum Research Fund Doctoral New Investigator Award, 3M Non-Tenured Faculty Award, University level Award of Excellence in Research & Scholarship, and College of Engineering Junior Faculty Research Excellence Award from University of Houston. Yu's recent research has been reported or highlighted by many media outlets, such as Time, Discovery, BBC News, NBC News, Science News, and USA Today.

Introduction

Paper is ubiquitous in our daily life and it is a renewable, abundant, and cheap flexible substrate material. Although it was originally invented for writing and recording purposes, with the fast technological development over the past century, the usage of paper has been broadly extended. For instance, paper has been employed as an effective platform for medical devices [1, 2, 3], electronics [4, 5, 6, 7], energy sources [8], etc. There are clear advantages when using paper as a substrate for these aforementioned applications, including low cost, scalability, manufacturability, degradability, and recyclability, compared with using other common candidates such as plastics and metal foils.

In particular, the past decade has witnessed extensive use of paper for various electronic devices and systems, such as diagnostic instruments [1, 2, 3], physical and chemical sensors [9, 10, 11, 12], circuits [13, 14], displays [5, 15], and energy sources [8]. Because of the compatibility and similarity between

paper manufacturing and device manufacturing, the associated low cost has been one of the driving forces in paper-based device development. For instance, Pollock et al. developed paper-based transaminase sensors for monitoring drug-induced liver injury [3]. Yang et al. developed a fully inkjet-printed gas sensor on a paper substrate [4]. Martins et al. developed complementary metal oxide semiconductor electronics on a flexible fiber-based paper substrate [14]. Andersson et al. fabricated an electrochromic display on a polymer-coated paper [5]. Hu et al. fabricated supercapacitors using paper composites inked with single-walled carbon nanotubes [16].

Among various electronic devices, the transistor is a fundamental building block for circuits and integrated systems to allow the functions of switching, interfacing, reading out, signal processing, etc. Paper-based transistors, in the format of thin-film transistors (TFTs), are therefore indispensable toward integrated paper electronic systems. Paper-based TFTs have been reported before [6, 7, 17, 18]. For instance, Zschieschang et al. developed an organic field effect transistor (OFET) on banknotes [6]. However, in the TFTs, paper was used solely as a supporting substrate, thus in a passive fashion for transistor-on-paper. Fortunato et al. and Lim et al. demonstrated paper transistors, where the papers were used not only as substrates but also as the gate dielectric [19, 20, 21]. However, the TFTs operated at relatively high voltages (tens of volts), which limits their potential practical applications, such as biomedical devices. The high operational voltage of paper TFTs is mainly due to the relatively low specific capacitance of the paper dielectric.

Here, we a present a flexible paper transistor in the format of transistor-in-paper with low operational voltage. Such a low operational voltage is a consequence of harnessing paper as the unique dielectric material in addition to its role as a natural substrate. Specifically, by taking advantage of the cellulose fiber microstructures of paper, we created an ion gel/cellulose fiber composite that serves as a dielectric once ion gels are added on the paper. The ion gel/cellulose fiber composite exhibits significantly increased specific capacitance, thus resulting in a much lower operational voltage of 1.8 V. The transistor-in-paper shows a high on/off current ratio of $\sim 10^4$ and retains transistor function even when it is bent. We further developed paper-based logic gates and a multiplexed active matrix tactile sensing mat device to show the capabilities and usages of the transistor-in-paper in electrical circuits. Detailed materials preparation, device fabrication, integration, and characterization illustrate the key aspects of the low-voltage transistor-in-paper and its potential usages in integrated paper electronic systems.

Results and discussion

One of the key steps for the transistor-in-paper fabrication involves the preparation of the ion gel/cellulose fiber composite. Figure 1(a) shows an optical image of the ion gel solution in a vial and the chemical compounds involved in its material preparation. Specifically, poly(vinylidene fluoride-*co*-hexafluoropropylene) [P(VDF-HFP)] and 1-ethyl-3-methylimidazolium tri(fluoromethanesulfonate) amide (EMIM-Otf) serve as the polymer matrix and ionic liquid, respectively. The ion gel preparation involves mixing the polymer matrix and the ionic liquid within acetone to first form a solution phase gel. The solution phase gel can be solidified upon thermal curing as described below. The detailed material preparation is described in the Materials and methods section. It is noted that the ion gel has poor adhesion with most substrates, such as plastics and metal foils. By taking advantage of the porous cellulose structure of paper (28 lbs, white, and brightness rating of 100 for sharp, Hammermill Paper Company, Pennsylvania), ion gel in liquid phase can first diffuse into paper and then solidify to form the composite of ion gel/cellulose fiber. It is noted that other papers with different porous cellulose architectures or different thickness could be used and their ion gel/cellulose fiber composite can be fabricated and optimized for low-voltage transistors. By using a stencil printing technique, ion gel can be selectively deposited onto the paper and the thickness of the composite after diffusion can be controlled. Figure 1(b) shows the cross-sectional image of the cellulose paper after stencil printing the ion gel solution onto the paper. A thin layer of ion gel diffused into the cellulose paper to form a ~30-μm-thick composite. The specific capacitances of the paper with and without loaded ion gel after solidification were characterized as a function of frequency. The imaginary impedance of the samples was first measured (Multi Autolab Cabinet, Metrohm, Herisau, Switzerland) by fixing the samples in between two parallel metal plates. The specific capacitance was calculated using the following equation:

$$C = 1/2A\pi fZ'' \quad , \tag{1}$$

where A is the sample surface area, f is frequency, and Z'' is the imaginary impedance. It should be noted that to form good contact with the metal plates, the samples were also coated with a thin layer of gold on the surfaces. The specific capacitance of the paper with ion gel increased from 0.34 to 21.5 nF/cm^2 at 1 Hz, as shown in Fig. 1(c). The specific capacitance increase of the paper after enhancement by the ion gel solution can be attributed to the high capacitance of the ion gel [22, 23, 24]. It is noted that the specific capacitance of the ion gel/cellulose fiber composite is lower than that of an ion gel dielectric. The reason is because the ion gel does not fully penetrate across the

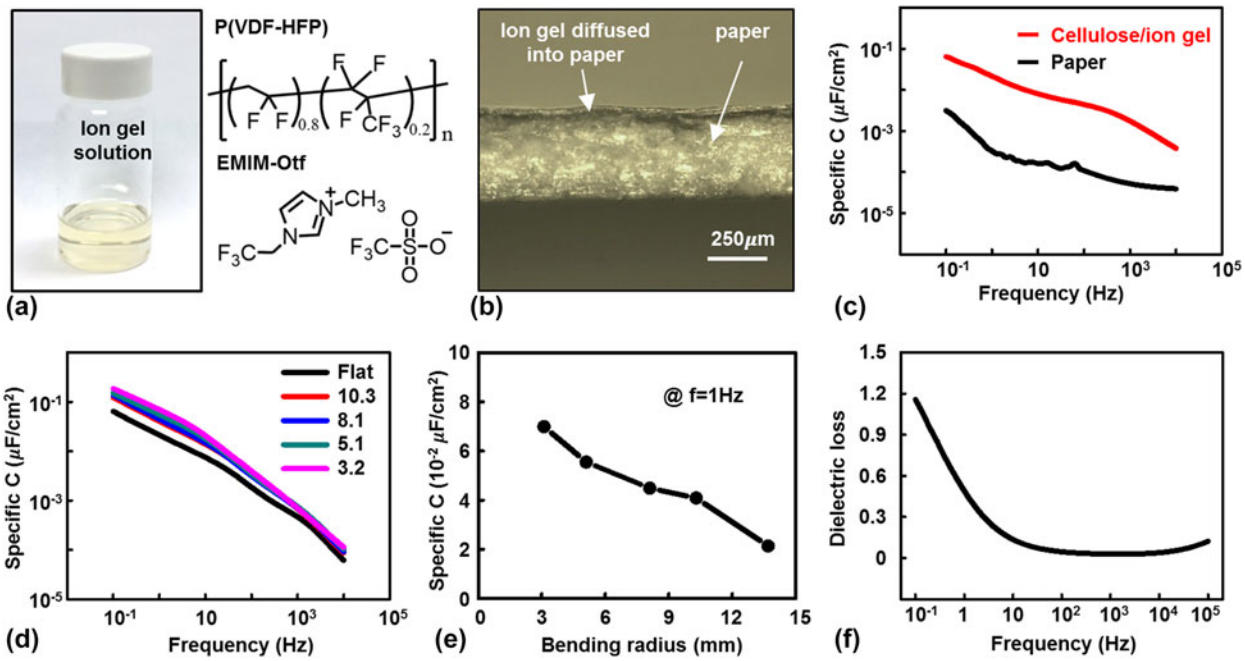

Figure 1: Characterization of the ion gel/cellulose fiber composite. (a) Optical image of the ion gel solution and its chemical compounds. (b) Optical image of the cross-sectional ion gel/cellulose fiber composite. (c) Specific capacitance of the paper and ion gel/cellulose fiber composite at different frequencies. Specific capacitance of the ion gel/cellulose fiber composite (d) under different frequencies and (e) under different bending radii at $f = 1$ Hz. (f) Dielectric loss of the ion gel/cellulose fiber composite under different frequencies.

thickness of the paper. Figure 1(d) shows the frequency-dependent specific capacitance of the ion gel/cellulose fiber composite under different bending radii. The specific capacitance of the composite increases as the bending radius decreases, and the specific capacitance at $f = 1$ Hz increased from 21.5 nF/cm^2 at the flat state to 69.9 nF/cm^2 at a bending radius of 3.2 mm, as shown in Fig. 1(e). The increased specific capacitance is attributed to the plastic deformation of the cellulose fibers and the reduced thickness of the fibers when they are bent. Figure 1(f) presents the frequency-dependent dielectric loss of the ion gel/cellulose composite.

The fabrication process of the flexible TFTs based on an ion gel/cellulose fiber composite is schematically illustrated in Fig. 2(a). Specifically, the process started with depositing the patterned indium gallium zinc oxide (IGZO) active layer, and Cr/Au source and drain electrodes through shadow masks, followed by stencil printing the ion gel and conductive rubber through shadow masks to serve as the dielectric and gate electrodes, respectively. The shadow masks were made of Kapton film, patterned by photolithography and dry etching, as reported in our prior work [25]. The preparation of the shadow masks is described in the Materials and methods section. Figure 2(b) shows the optical image of the bendable transistor-in-paper. The transistor was devised into a back gated structure. The schematic structure is shown in Fig. 2(c). The channel length and width of the TFTs are 50 μm and 2 mm, respectively. Figures 2(d) and 2(e) show the SEM images of the cellulose paper before and after IGZO deposition. As can be seen, the fibers are covered with the IGZO film that remains continuous even after bending, which ensures that the transistor retains its electrical functions.

The forward and backward swept transfer characteristics ($I_D - V_{GS}$, in black) of the ion gel/cellulose fiber composite–based transistor-in-paper are shown in Fig. 3(a). The drain current was measured while sweeping V_{GS} from −0.6 to 4 V at a constant V_{DS} of 1 V. The transistor operated in the enhancement mode with a low drain current at $V_{GS} = 1.2$ V and showed a reasonable on/off current ratio of $\sim 10^4$, which is comparable to that of IGZO-based TFTs on paper substrates [7, 18, 19]. The field effect mobility of the transistor was calculated from the slope in the saturation regime of the square root of the drain current versus the gate voltage [Fig. 3(a), red]. The mobility was then calculated based on the following equation [26, 27, 28] for the transistor working in the saturation region:

$$I_D = \frac{WC_i}{2L}\mu(V_G - V_T)^2 \quad ,$$

where C_i (21.5 nF/cm^2) is the specific capacitance chosen at the frequency of 1 Hz, W (2 mm) is the channel width, L (50 μm) is the channel length, and V_T is the threshold voltage. It is noted that the specific capacitance at low frequencies was used to avoid overestimation of the mobility due to the low

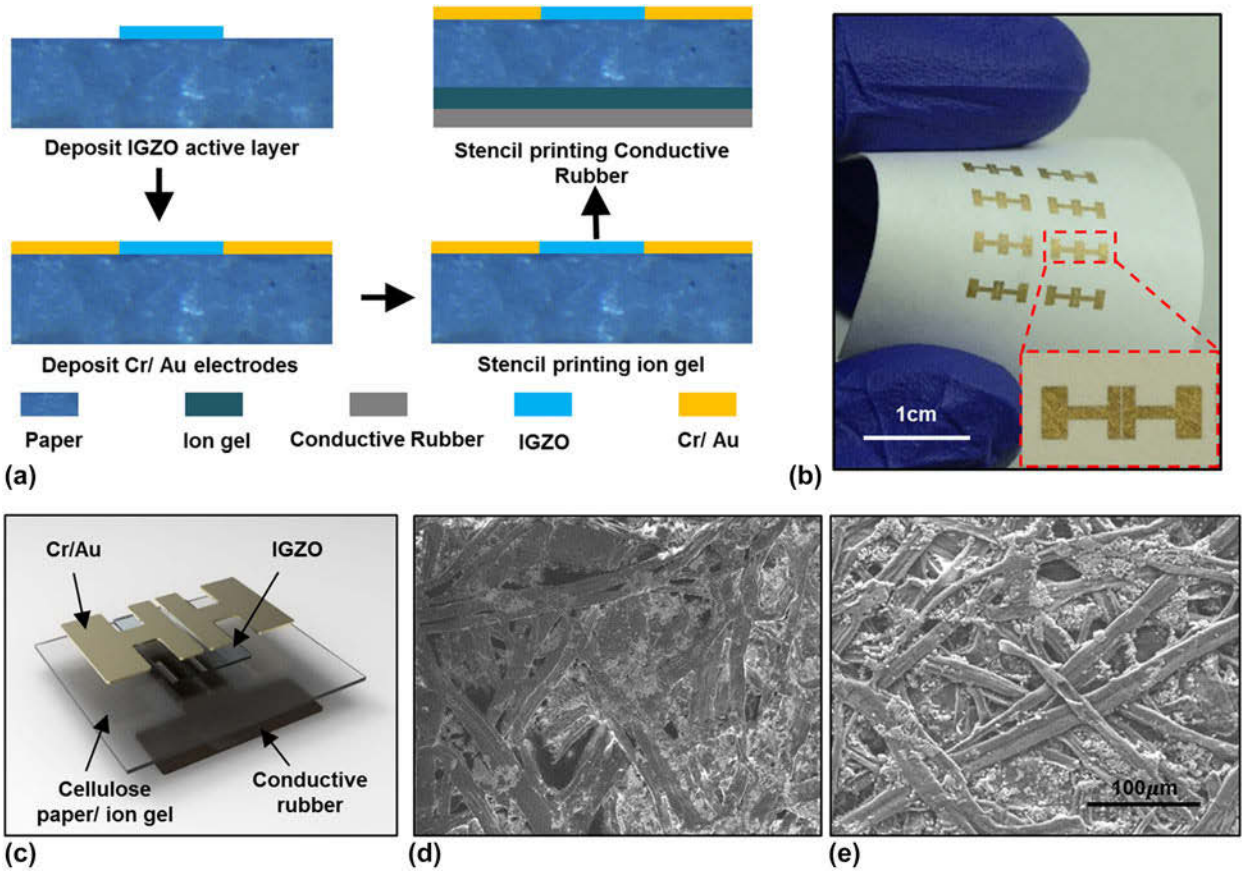

Figure 2: Flexible low-voltage transistor-in-paper. (a) The fabrication process, (b) optical image, and (c) schematic structure of the transistors based on ion gel/cellulose fiber composite. SEM images of cellulose paper (d) before and (e) after depositing the IGZO semiconductor layer.

capacitance at high frequencies. The saturation mobility was calculated to be 9.1 $cm^2/(V\ s)$. As a comparison, the transfer curve of a paper transistor without the addition of ion gel is shown in Fig. 3(b), where the operation voltage is about 10 V, much higher than that of the transistor-in-paper. The calculated mobility of the transistor without the addition of ion gel is 8.7 $cm^2/(V\ s)$. These calculations suggest comparable results for the IGZO thin-film transistor [7, 19, 21]. It is noted that the ion gel/cellulose fiber–based device does not show any transistor characteristics at low gate voltage <5 V. Figure 3(c) shows the output characteristics (I_D–V_{DS}) of the transistor-in-paper at different gate voltages (V_{GS}), ranging from 2 to 5 V with a voltage step of 0.3 V. The drain voltage was increased from 0 to 1 V. The output characteristics indicate an increase in channel conductance with increased V_{GS}. Saturation in the drain current was observed in the high drain voltage regime. A saturation current as high as 20 μA was obtained at V_{GS} = 5 V and V_{DS} = 1 V. The threshold voltage decreased to 1.8 V, compared with V_T = 10 V for transistor-on-paper without ion gel as mentioned previously. Such a significant decrease in the threshold voltage is due to the larger capacitance of the ion gel/cellulose fiber composite.

The device performance upon mechanical bending was also characterized. The set of transfer curves, shown in Fig. 3(d), indicate that there was no significant performance degradation for the TFTs of which the bending radii are larger than 5.1 mm. The bending direction was aligned with the channel length direction to achieve the maximum applied mechanical strain on the device. As the bending radius decreased to 3.2 mm, only a slight decrease in the on-current was observed. These results suggest that the flexible low-voltage transistor-in-paper is robust to bending.

We further developed a flexible ion gel/cellulose fiber composite–based inverter to illustrate digital logic gate functions. The inverter is a basic component for various digital and integrated circuits. Two types of inverters, including a diode-load inverter and a zero-V_{GS} inverter, were constructed [29]. Figures 4(a) and 4(b) show the schematic structure and equivalent circuit diagram of the diode-load inverter. The transistors in the inverter had a channel length of 50 μm. The channel width of the driving TFT in the diode-load inverter and that of the loading TFT in the zero-V_{GS} inverter was 2 mm. The channel width ratio of the loading TFT and the driving TFT in the diode-load inverter was 1/3. Figure 4(c)

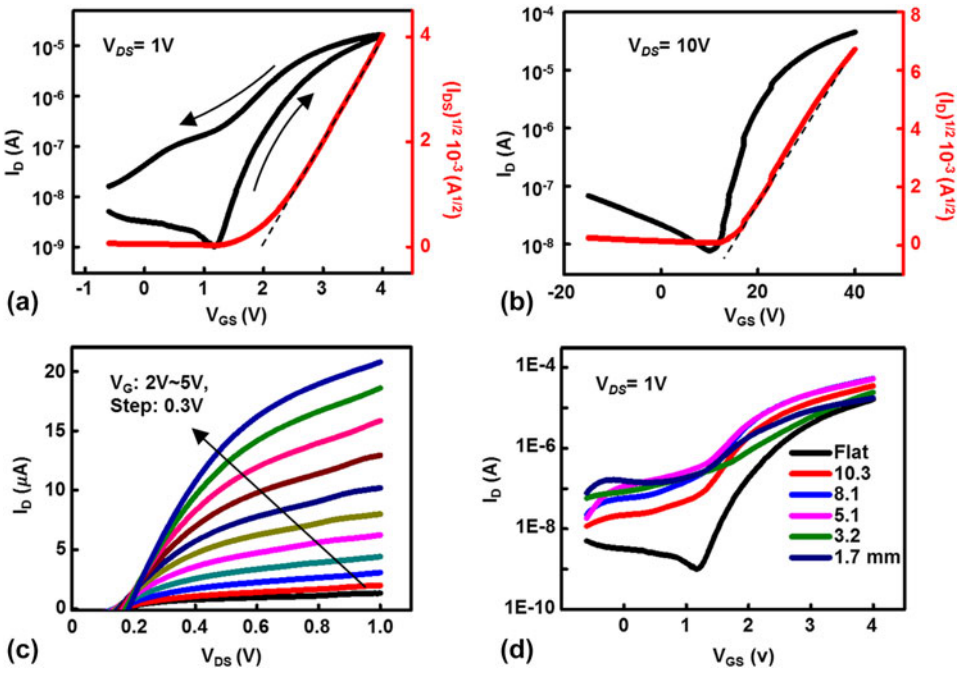

Figure 3: Characterization of the low-voltage transistor-in-paper. (a) Forward and backward transfer curves of TFTs based on ion gel/cellulose fiber composite. The red curve corresponds to the forward transfer curve. (b) Transfer curve of TFTs based on cellulose fiber paper. (c) Output curves of TFTs on ion gel/cellulose fiber composite. (d) Transfer curves of the TFTs on ion gel/cellulose fiber composite under different bending radii.

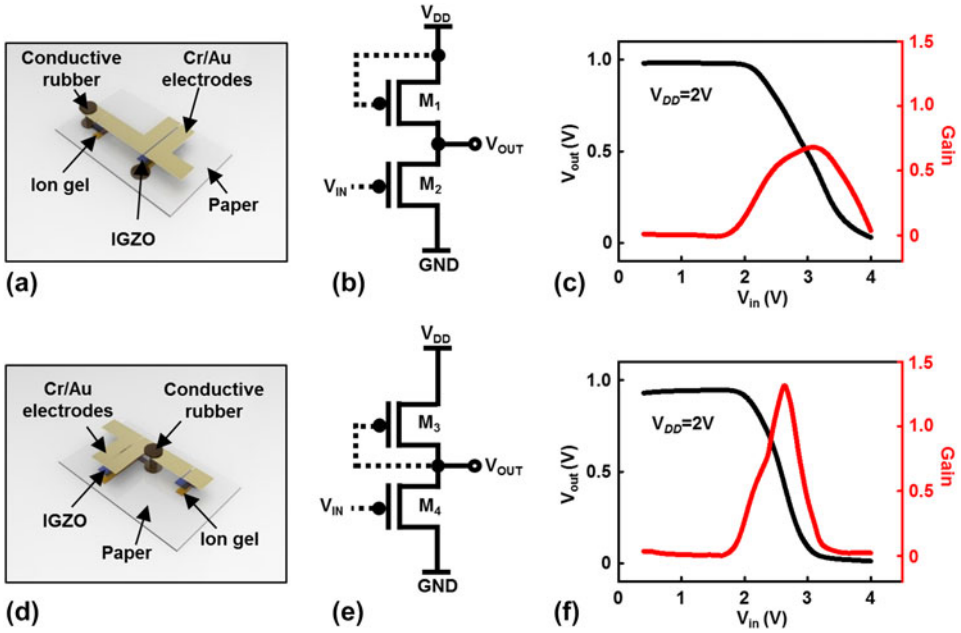

Figure 4: Characterization of paper transistor–based inverters. (a) Schematic structure, (b) equivalent circuit diagram, and (c) VTC of the diode-load inverter. Channel width ratio $\beta_1 = (W_1/W_2) \sim (1/3)$. (d) Schematic structure, (e) equivalent circuit diagram, and (f) VTC of the zero-V_{GS} inverter. Channel width ratio $\beta_2 = (W_3/W_4) \sim (3/1)$.

shows the measured voltage transfer curves (VTCs) and gains of the diode-load inverter while V_{DD} was kept at 2 V. Figures 4(d) and 4(e) show the schematic structure and equivalent circuit diagram of the zero-V_{GS} inverter, respectively. The channel length of the transistor was 50 μm. The channel width of the loading TFT in the zero-V_{GS} inverter was 2 mm. The channel width ratio of the loading TFT and the driving TFT in the zero-V_{GS} inverter was 3/1. Figure 4(f) shows the measured VTC curve and gain of the zero-V_{GS} inverter. Both types of inverters showed adequate voltage transfer. The

gain of the diode-load inverter and that of the zero-V_{GS} inverter were about 0.7 and 1.3, respectively, which are comparable to those of IGZO-based inverters on plastic substrates [29].

Transistors are the basis for multiplexed active matrix arrays which are useful for many applications, such as pixel addressing and spatial and temporal sensing. Flexible transistor-in-paper offers the multiplexing capabilities in paper integrated devices. We developed a flexible tactile sensing mat with multiplexing readout capabilities based on a 5 × 5 array of ion gel/cellulose fiber composite–based transistors. The tactile sensing mat was composed of a piece of pressure-sensitive rubber (PSR) and an array of transistor-in-paper, where the PSR served as a pressure-sensitive component and the transistors were multiplexing units, respectively. Figure 5(a) shows the schematic structure of the pressure sensing mat in layered exploded view. Figure 5(b) presents the optical image of the top side of the device. The mat was accomplished through integrating the PSR onto the prefabricated transistor array. The detailed fabrication process of the mat is described in the Materials and methods section. Figure 5(c) depicts a photo of the mat device. Since every component, including the transistor and PSR, is soft and flexible, the entire mat device is also flexible. The detailed multiplex array is schematically illustrated by the circuit diagram in Fig. 5(d). The PSR acts a variable resistor upon different applied pressures. Each tactile sensing node was connected through an ion gel/cellulose dielectric–based paper transistor in the array. The gate electrodes of each line were connected to a word line (V_{WL}), whereas the drain electrodes of each line were connected to a bit line (V_{BL}) [30].

The electrical resistance of the PSR changed under applied pressure. The PSR had a threshold pressure of ~94 kPa. As a pressure higher than 94 kPa was applied on the mat, the resistance of the PSR varied from several GΩ at a nonpressed state to several Ω at a pressed state [31]. The circuit diagram of each sensing node of the pressure sensing mat is shown in Fig. 6(a). The drain current (I_D) dependence on the gate voltage (V_{GS}) at different states is shown in Fig. 6(b). A pressure map therefore can be obtained by multiplexed readout of the output current of the channels with applied voltages of V_{DS} = 1 V for each bit line and V_{GS} = 4 V for each word line. Figure 6(c) shows the current output of the mat upon applying pressure using triangular and rectangular objects. The pressed sensors have a high drain current output of up to 10^{-5} A, whereas nonpressed sensing nodes have a relatively low drain current output of around 10^{-11} A. These results indicate that the array of ion gel/cellulose dielectric–based transistor-in-paper can successfully serve as a multiplexing readout circuit. It is noted

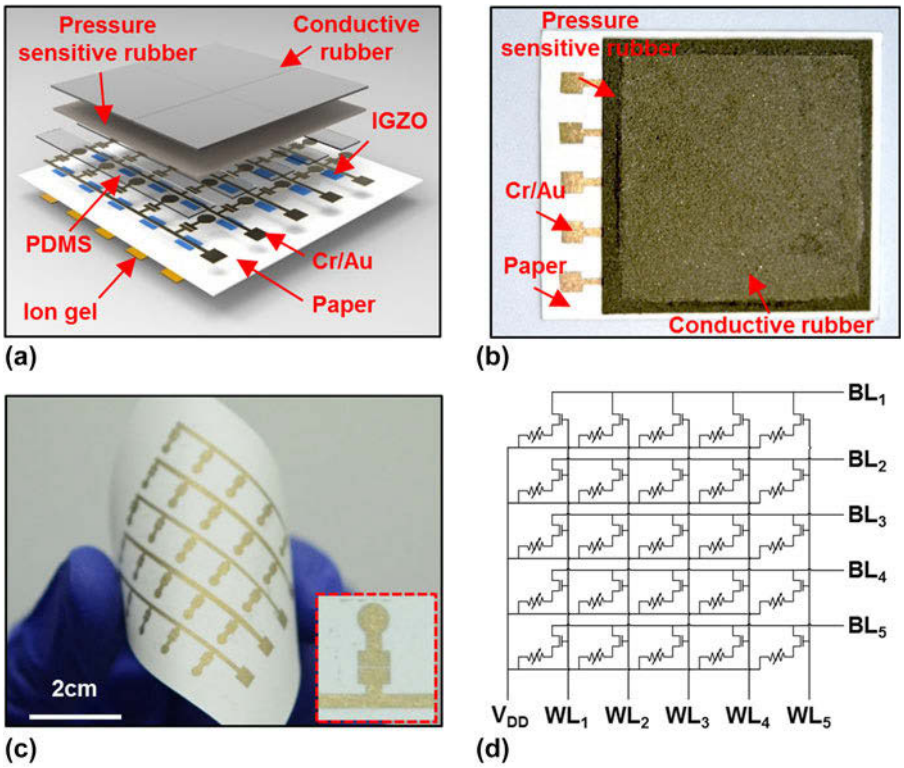

Figure 5: Design and structures of active matrix based multiplexed tactile sensing mat. (a) Schematic structure and (b) optical image of the tactile sensing mat. (c) Optical image of the flexible transistor array for building the active matrix multiplexed sensing mat. (d) Circuit diagram of the 5 × 5 tactile sensing mat.

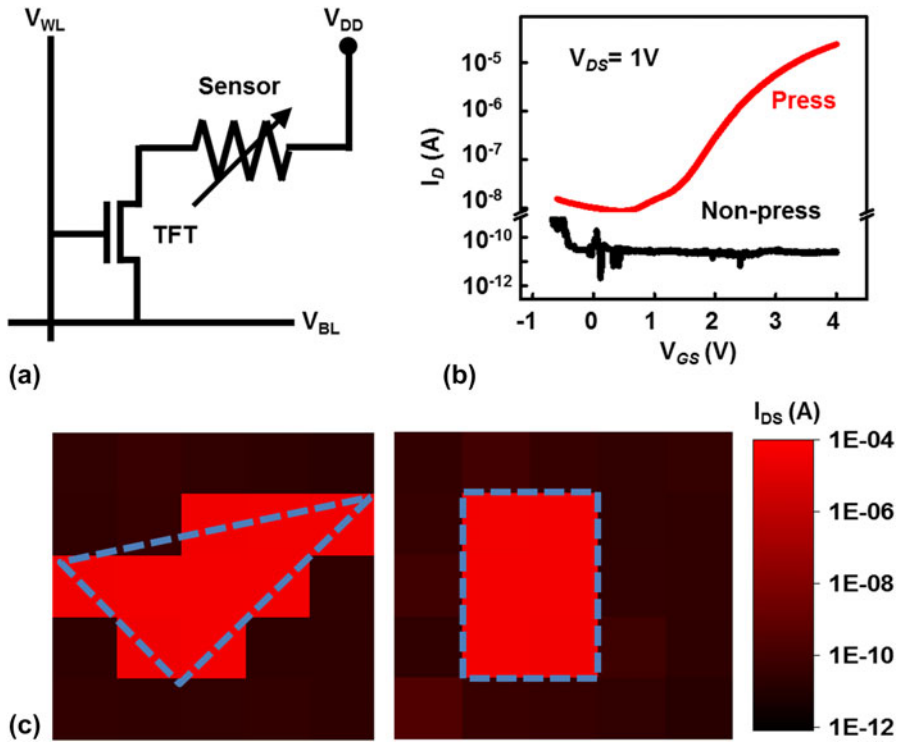

Figure 6: Characteristics of the tactile sensing mat. (a) Circuit diagram of each sensing node. V_{BL}, bit line; V_{WL}, word line; V_{DD}, supply voltage. (b) Transfer curves of a single pixel in the matrix at a pressed state and at a nonpressed state. (c) Current mapping of the tactile sensing mat with applied pressure using triangular-shaped (left) and rectangular-shaped (right) objects.

that the resolution of the tactile sensing mat can be further improved through optimizing the design of the transistor array.

Conclusions

In conclusion, we developed a flexible low-voltage transistor-in-paper, where the paper served as the substrate and also the dielectric in a format of an ion gel composite. Owing to the porous cellulose structure of the paper, ion gel was partially embedded into the paper and formed composite with very high specific capacitance (21.5 nF/cm^2). Such an ion gel/cellulose fiber composite substrate gave rise to the low-threshold voltage of the transistor. By taking advantage of the various additive manufacturing means for semiconductors and conductors, a flexible transistor was simply constructed and retained robust performance. The flexible low-voltage transistor-in-paper was utilized to build digital logic circuits and integrated electronics functions. As demonstrated in this work, inverters and active matrix multiplexing arrays were developed. An active matrix array based on the ion gel/cellulose fiber composite could be immediately used for arrayed sensing readout, as exemplified by the tactile sensing mat. All the results show that the ion gel–modified paper renders a class of promising, flexible, low-voltage transistors and circuits that can be potentially integrated toward the development of integrated paper electronic devices and systems, medical devices, human–machine interfaces, etc. Modification of the paper cellulose structures sheds light on future development of various paper devices.

Materials and methods

Preparation of ion gel dielectric solution

The ion gel dielectric solution was obtained by mixing P(VDF-HFP) (M_w ~ 400,000, Sigma-Aldrich, Missouri), ionic liquid EMIM-Otf (>98%, Sigma-Aldrich, Missouri), and acetone (>99.9%, Sigma-Aldrich, Missouri) at a weight ratio of 1:4:7 at 70 °C.

Preparation of the ion gel/cellulose fiber composite

The ion gel/cellulose fiber composite was prepared by stencil printing the ion gel solution on the cellulose paper (28 lbs, white, and brightness rating of 100 for sharp, Hammermill Paper Company, Pennsylvania), using a razor blade, followed by curing in a vacuum oven at 70 °C for 12 h to solidify.

Shadow mask preparation

The shadow masks were made of Kapton film (25.4 μm thick, Dupont, Delaware). The preparation of shadow mask began with spin-coating (1000 rounds per minute for 30 s, Brewer

Cee 200 spin coater, Brewer Science Inc., Missouri) a thin layer of PDMS on a cleaned glass slide and curing to form an adhesive layer. A piece of Kapton film was laminated onto the PDMS surface and dehydrated at 90 °C for 10 min after cleaning the film surface. Then, a layer of 500-nm-thick Cu was deposited on top of the Kapton film using electron-beam evaporation (Thermionics, Washington), followed by patterning the Cu through photolithography and wet etching. Reactive ion etching (oxygen: 40 standard cubic centimeter per minute; power, 250 W; Oxford plasma lab 80 plus, Oxford Instruments, Abingdon, United Kingdom) was performed for 8 h to etch through the Kapton film. Then the completed shadow mask was peeled off from the PDMS adhesive.

Fabrication of the ion gel/cellulose fiber composite–based flexible TFTs

The ion gel/cellulose fiber composite–based TFTs were fabricated by first depositing IGZO (30 nm, Kurt J. Lesker, Pennsylvania) on the cellulose paper by DC sputtering (20 W; 50 mtorr, 10% of oxygen partial pressure to argon, with source to substrate distance of around 17 cm, AJA ATC 2200 UHV sputtering system, AJA International Inc., Massachusetts) through shadow masks. Then, the Cr/Au (5 nm/60 nm) source and drain electrodes were formed by e-beam evaporation through the shadow mask, followed by stencil printing the ion gel. Finally, conductive rubber (Zoflex, FL45) was stencil-printed on the ion gel/cellulose fiber composite substrate as the bottom gate.

Fabrication of the ion gel/cellulose fiber composite–based tactile sensing mat

The fabrication process of the pressure sensor matrix involved fabricating the TFT array on an ion gel/cellulose fiber composite substrate, covering the source electrodes of the TFT array using polydimethylsiloxane (PDMS, Dow-Corning, Michigan), and laminating the PSR covered by conductive rubber onto the TFT array. The TFT array was fabricated in the same way as that of the TFTs on the ion gel/cellulose fiber composite substrate. Then, a PDMS insulating layer was scratch-coated on the TFT array through shadow masks followed by coating conductive rubber on the source electrodes of the TFTs. Finally, the PSR (Zoflex, ZL45.1) coated with the conductive rubber paste (Zoflex, FL45) was laminated on top of the device.

Material characterization and device measurements

An optical microscope (Eclipse LV100ND, Nikon, Tokyo, Japan) was used to capture the optical images of the cross-sectional structure of the ion gel/cellulose fiber composite. The frequency-dependent specific capacitances of the cellulose paper and ion gel/cellulose fiber composite were measured by an impedance analyzer (Multi Autolab Cabinet, Metrohm, Herisau, Switzerland). The electrical properties of the transistors, inverters, and pressure sensor matrix were characterized by a semiconductor analyzer (4200SCS, Keithley Instruments Inc., Ohio).

Acknowledgments

C.Y. would like to acknowledge the funding supports from the NSF ECCS award (No. 1509763), Doctoral New Investigator grant from American Chemical Society Petroleum Research Fund (56840-DNI7), 3M nontenured faculty award, and the startup fund from University of Houston.

References

1. **A.W. Martinez, S.T. Phillips, E. Carrilho, S.W. Thomas, III, H. Sindi, and G.M. Whitesides**: Simple telemedicine for developing regions: Camera phones and paper-based microfluidic devices for real-time, off-site diagnosis. *Anal. Chem.* **80**, 3699–3707 (2008).
2. **A.W. Martinez, S.T. Phillips, G.M. Whitesides, and E. Carrilho**: Diagnostics for the developing world: Microfluidic paper-based analytical devices. *Anal. Chem.* **82**, 3–10 (2009).
3. **N.R. Pollock, J.P. Rolland, S. Kumar, P.D. Beattie, S. Jain, F. Noubary, V.L. Wong, R.A. Pohlmann, U.S. Ryan, and G.M. Whitesides**: A paper-based multiplexed transaminase test for low-cost, point-of-care liver function testing. *Sci. Transl. Med.* **4**, 152ra129 (2012).
4. **L. Yang, R. Zhang, D. Staiculescu, C. Wong, and M.M. Tentzeris**: A novel conformal RFID-enabled module utilizing inkjet-printed antennas and carbon nanotubes for gas-detection applications. *IEEE Antennas Wirel. Propag. Lett.* **8**, 653–656 (2009).
5. **P. Andersson, D. Nilsson, P.O. Svensson, M. Chen, A. Malmström, T. Remonen, T. Kugler, and M. Berggren**: Active matrix displays based on all-organic electrochemical smart pixels printed on paper. *Adv. Mater.* **14**, 1460–1464 (2002).
6. **U. Zschieschang, T. Yamamoto, K. Takimiya, H. Kuwabara, M. Ikeda, T. Sekitani, T. Someya, and H. Klauk**: Organic electronics on banknotes. *Adv. Mater.* **23**, 654–658 (2011).
7. **W. Lim, E.A. Douglas, D.P. Norton, S.J. Pearton, F. Ren, Y.W. Heo, S.Y. Son, and J.H. Yuh**: Low-voltage indium gallium zinc oxide thin film transistors on paper substrates. *Appl. Phys. Lett.* **96**, 053510 (2010).
8. **L. Jabbour, R. Bongiovanni, D. Chaussy, C. Gerbaldi, and D. Beneventi**: Cellulose-based Li-ion batteries: A review. *Cellulose* **20**, 1523–1545 (2013).

9. **L. Yang, A. Rida, R. Vyas, and M.M. Tentzeris**: RFID tag and RF structures on a paper substrate using inkjet-printing technology. *IEEE Trans. Microwave Theory Tech.* **55**, 2894–2901 (2007).
10. **R. Vyas, V. Lakafosis, A. Rida, N. Chaisilwattana, S. Travis, J. Pan, and M.M. Tentzeris**: Paper-based RFID-enabled wireless platforms for sensing applications. *IEEE Trans. Microwave Theory Tech.* **57**, 1370–1382 (2009).
11. **V. Lakafosis, A. Rida, R. Vyas, L. Yang, S. Nikolaou, and M.M. Tentzeris**: Progress towards the first wireless sensor networks consisting of inkjet-printed, paper-based RFID-enabled sensor tags. *Proc. IEEE* **98**, 1601–1609 (2010).
12. **E.W. Nery and L.T. Kubota**: Sensing approaches on paper-based devices: A review. *Anal. Bioanal. Chem.* **405**, 7573–7595 (2013).
13. **D.H. Kim, Y.S. Kim, J. Wu, Z. Liu, J. Song, H.S. Kim, Y.Y. Huang, K.C. Hwang, and J.A. Rogers**: Ultrathin silicon circuits with strain-isolation layers and mesh layouts for high-performance electronics on fabric, vinyl, leather, and paper. *Adv. Mater.* **21**, 3703–3707 (2009).
14. **R. Martins, A. Nathan, R. Barros, L. Pereira, P. Barquinha, N. Correia, R. Costa, A. Ahnood, I. Ferreira, and E. Fortunato**: Complementary metal oxide semiconductor technology with and on paper. *Adv. Mater.* **23**, 4491–4496 (2011).
15. **J.Y. Kim, S.H. Park, T. Jeong, M.J. Bae, S. Song, J. Lee, I.T. Han, D. Jung, and S. Yu**: Paper as a substrate for inorganic powder electroluminescence devices. *IEEE Trans. Electron Devices* **57**, 1470–1474 (2010).
16. **L. Hu, J.W. Choi, Y. Yang, S. Jeong, F. La Mantia, L.F. Cui, and Y. Cui**: Highly conductive paper for energy-storage devices. *Proc. Natl. Acad. Sci.* **106**, 21490–21494 (2009).
17. **H. Shin, J. Roh, J. Song, H. Roh, C.M. Kang, T. Lee, G. Park, K. An, J.Y. Kim, H. Kim, and J. Kwak**: Highly stable organic transistors on paper enabled by a simple and universal surface planarization method. *Adv. Mater. Interfaces* **6**, 1801731 (2019).
18. **G. Grau, E.J. Frazier, and V. Subramanian**: Printed unmanned aerial vehicles using paper-based electroactive polymer actuators and organic ion gel transistors. *Microsyst. Nanoeng.* **2**, 16032 (2016).
19. **E. Fortunato, N. Correia, P. Barquinha, L. Pereira, G. Gonçalves, and R. Martins**: High-performance flexible hybrid field-effect transistors based on cellulose fiber paper. *IEEE Electron Device Lett.* **29**, 988–990 (2008).
20. **R. Martins, P. Barquinha, L. Pereira, N. Correia, G. Gonçalves, I. Ferreira, and E. Fortunato**: Write-erase and read paper memory transistor. *Appl. Phys. Lett.* **93**, 203501 (2008).
21. **W. Lim, E.A. Douglas, S.H. Kim, D.P. Norton, S.J. Pearton, F. Ren, H. Shen, and W.H. Chang**: High mobility $InGaZnO_4$ thin-film transistors on paper. *Appl. Phys. Lett.* **94**, 072103 (2009).
22. **M.L. Hammock, A. Chortos, B.C.K. Tee, J.B.H. Tok, and Z. Bao**: 25th anniversary article: The evolution of electronic skin (e-skin): A brief history, design considerations, and recent progress. *Adv. Mater.* **25**, 5997–6038 (2013).
23. **J.H. Cho, J. Lee, Y. Xia, B. Kim, Y. He, M.J. Renn, T.P. Lodge, and C.D. Frisbie**: Printable ion-gel gate dielectrics for low-voltage polymer thin-film transistors on plastic. *Nat. Mater.* **7**, 900 (2008).
24. **K.H. Lee, M.S. Kang, S. Zhang, Y. Gu, T.P. Lodge, and C.D. Frisbie**: "Cut and stick" rubbery ion gels as high capacitance gate dielectrics. *Adv. Mater.* **24**, 4457–4462 (2012).
25. **Y. Gao, Y. Zhang, X. Wang, K. Sim, J. Liu, J. Chen, X. Feng, H. Xu, and C. Yu**: Moisture-triggered physically transient electronics. *Sci. Adv.* **3**, e1701222 (2017).
26. **S.D. Brotherton**: *Introduction to Thin Film Transistors: Physics and Technology of TFTs* (Springer Science & Business Media, Switzerland, 2013).
27. **J.S. Lee, S. Chang, S.M. Koo, and S.Y. Lee**: High-performance a-IGZO TFT with ZrO_2 gate dielectric fabricated at room temperature. *IEEE Electron Device Lett.* **31**, 225–227 (2010).
28. **H. Yabuta, M. Sano, K. Abe, T. Aiba, T. Den, H. Kumomi, K. Nomura, T. Kamiya, and H. Hosono**: High-mobility thin-film transistor with amorphous $InGaZnO_4$ channel fabricated by room temperature rf-magnetron sputtering. *Appl. Phys. Lett.* **89**, 112123 (2006).
29. **T.C. Huang, K. Fukuda, C.M. Lo, Y.H. Yeh, T. Sekitani, T. Someya, and K.T. Cheng**: Pseudo-CMOS: A design style for low-cost and robust flexible electronics. *IEEE Trans. Electron Devices* **58**, 141–150 (2011).
30. **T. Someya, T. Sekitani, S. Iba, Y. Kato, H. Kawaguchi, and T. Sakurai**: A large-area, flexible pressure sensor matrix with organic field-effect transistors for artificial skin applications. *Proc. Natl. Acad. Sci. U. S. A.* **101**, 9966–9970 (2004).
31. **K. Sim, Z. Rao, H.J. Kim, A. Thukral, H. Shim, and C. Yu**: Fully rubbery integrated electronics from high effective mobility intrinsically stretchable semiconductors. *Sci. Adv.* **5**, eaav5749 (2019).